J/Ψ production in deep inelastic electron scattering at HERA

Lennart Zwirner

II. Institut für Theoretische Physik, Universität Hamburg, Luruper Chaussee 149, D-22761 Hamburg, Germany

E-mail: zwirner@mail.desy.de

Abstract. J/ψ production in deep inelasic electron proton scattering is calculated in the framework of nonrelativistic quantum chromodynamics. All the calculated differential distributions, except for one, turn out to be very sensitive to the color octet mechanism. The analytic results disagree with previous analyses, both for the colour singlet and colour octet channels. The theoretical predictions agree reasonably well with recent data taken by the H1 Collaboration at DESY HERA, significantly better than those obtained within the colour singlet model.

1. Introduction

In high energy collisions, resonances are observable, which after the advent of the parton model and QCD could be identified as strongly bound states of quark antiquark pairs, so called quarkonia, with specific radial excitation, spin and orbital angular momentum quantum numbers

$$n_r \, {}^{2S+1}L_J \quad , \quad n_r = 1, 2, 3, ... \quad ,$$

where through this talk the conventional spectroscopic notation is used. Some representatives of the heavy quarkonia ($q\bar{q}$ with $q = c, b, t$) are:

	q	n_r	${}^{2S+1}L_J$
η_c	c	1	${}^1S_0$
h_c	c	1	${}^1P_1$
J/Ψ	c	1	${}^3S_1$
Ψ'	c	2	${}^3S_1$
χ_{cJ}	c	1	${}^3P_J$
Υ	b	1	${}^3S_1$
χ_{bJ}	b	1	${}^3P_J$

As the simplest strongly bound systems with a rich internal structure, they provide an important testing ground for QCD. Heavy quarkonia are particularly suited to investigate the interesting interplay between perturbative and nonperturbative aspects of QCD. Special attention is paid to the J/Ψ owing to its very clean experimental signature of leptonic decay. The topic of this talk is the prediction of J/Ψ electroproduction at DESY HERA in the framework of nonrelativistic QCD [1]. This process is very important for studying the quarkonium production mechanism because, in contrast to photoproduction, which lacks any higher scale other than the J/Ψ mass, in deep inelastic scattering the photon virtuality Q^2 provides a high scale, by which higher order corrections and nonperturbative contributions like higher twist effects are effectively suppressed. An additional advantage is, that for high Q^2 the contribution of resolved photons becomes neglegible, rendering the calculation independent from theoretical uncertainties in the photon structure functions. Before presenting the calculation, it is necessary to give a brief overview over the theoretical concepts and models, on which such calculations rely.

2. Factorization approaches to quarkonium physics

2.1. Factorization

Production and decay of heavy quarkonia involve highly nonperturbative dynamics related to the quarkonium binding state. Therefore, theoretical approaches to quarkonium physics in general rely on a factorization of observables like production or decay rates into nonperturbative parameters, which must be determined phenomenologically, and coefficients, which are calculable within perturbation theory. The parameters contain all the nonrelativistic effects at long distances comparable to the quarkonium binding length, which by the Heisenberg uncertainty principle is nearly the inverse of the heavy quark relative momentum $m_q v$, m_q being the heavy quark mass and v the heavy quark relative velocity in the quarkonium rest frame, while the coefficients describe the relativistic dynamics at a short distance scale, which analogously is estimated to be $\frac{1}{m_q}$, the inverse of the magnitude of the typically involved relativistic momenta. Hence the criterion for the reliability of such a factorization is the smallness of v. Only for $v \ll 1$ the scales of the short distance and the long distance dynamics are well separated $\frac{1}{m_q} \ll \frac{1}{m_q v}$. The long distance process then cannot be significantly influenced by the short distance process, implying universality of the matrix elements: Once one has extracted them from one special process, they should be valid for any other process. This constitutes the predictive power of the theory. With $v^2 \sim 0.3$ the charmonia are the lightest quarkonia, which accomplish the condition for such a factorization approach.

2.2. The Color Singlet Model (CSM)

The conventional picture of heavy quarkonium production and decay based on such a factorization assumption is the Color Singlet Model (CSM) [2]. In this model, the perturbative short distance part of the cross section describes the creation of a heavy quark antiquark pair in a color singlet state with exactly the spin angular momentum quantum numbers of the observed quarkonium, while the nonperturbative long distance part corresponds to the transition of this state into the physical quarkonium binding state. A similar factorization applies to the decay rate.

2.3. NRQCD

Nonrelativistic QCD (NRQCD) [3] is an effective theory of heavy quarkonia, putting the factorization approach onto a rigid field theoretic basis. It relies on a Lagrangian, which treats the heavy quark degrees of freedom nonrelativistically and takes relativistic corrections order by order into account, while the light degrees of freedom are still described by full relativistic QCD. Heavy quarkonium production and decay rates are given by factorization formulas, which accord to a generalization of the CSM. The intermediate heavy quark pair is now also allowed to acquire quantum numbers different from those of the physical quarkonium. In particular, it may even occur in a color octet state, whereby the subsequent formation of the binding state must then be accompanied by some mechanism of color compensation like soft gluon emission. This Color Octet Mechanism (COM) is an essential novelty compared to the conventional CSM. The NRQCD factorization formulas explicitly read for the production cross section

$$\sigma(ij \to QX) = \sum_n \hat{\sigma}\left(ij \to q\bar{q}[n]\right) \left\langle 0|O_n^Q|0\right\rangle \tag{1}$$

and for the decay rate

$$\Gamma(Q \to X) = \sum_n \hat{\Gamma}\left(q\bar{q}[n] \to X\right) \left\langle 0|O_Q^n|0\right\rangle \quad . \tag{2}$$

The summation in both cases extends over all $n = \left[1/8,^{2S+1} L_J\right]$, 1,8 denoting a color singlet or color octet state respectively and $^{2S+1}L_J$ being the spectroscopic notation for the spin angular momentum quantum numbers. $\sigma(ij \to q\bar{q}[n])$ are the perturbative coefficients , describing the creation of the heavy quark pair in the quantum state n and $\left\langle 0|O_n^Q|0\right\rangle$ are the NRQCD production matrix elements, which parametrize the nonperturbative transition of this state into the quarkonium Q. Analogously $\left\langle 0|O_Q^n|0\right\rangle$ are the NRQCD decay matrix elements, corresponding to the probability to meet the heavy quark pair in the quarkonium Q in a Fock state of quantum numbers n while $\hat{\Gamma}\left(q\bar{q}[n] \to X\right)$ are the perturbative coefficients, which describe the annihilation of the heavy quark pair in this state.

In principle the NRQCD factorization formulas are sums of infinitely many terms. However, the NRQCD matrix elements scale in a well defined manner with powers of the heavy quark relative velocity v [3]. Therefore the sums in eqs. (1),(2) can in general

be amputated after the first leading terms. In the case of J/Ψ for example, the only relevant matrix elements within the limits of the current experimental accuracy are those belonging to

$$n = \left[1,^3 S_1\right] \ , \ \left[8,^1 S_0\right] \ , \ \left[8,^3 S_1\right] \ , \ \left[8,^3 P_J\right] \ .$$

For S wave quarkonia the NRQCD factorization approach reduces in the limit of vanishing v to the CSM.

2.4. NRQCD versus CSM

Within NRQCD serious problems of the CSM are resolved. The CSM underestimates the J/Ψ production rate at the Tevatron measured by the CDF collaboration by a factor of $20 - 50$ [4]. In the framework of NRQCD this discrepancy could be eliminated by including the color octet contributions: At large p_T values, J/Ψ production at the Tevatron was found to be dominated by gluon fragmentation [5]. Secondly, different from the CSM, NRQCD allows for the infrared safe calculation of the decay of P wave quarkonia, such as h_c or χ_{cJ}, since the divergencies occuring in the color singlet channel ($[1^1P_1]$ for h_c, $[1^3P_J]$ for χ_{cJ}) are cancelled by those in the color octet channel ($[8^1S_0]$ for h_c, $[8^3S_1]$ for χ_{cJ}) [6].

3. NRQCD analysis of J/Ψ production in deep inelastic electron scattering at HERA

3.1. The analytical calculation

An NRQCD calculation of J/Ψ electroproduction was performed including, besides the leading color singlet contribution, all the color octet channels up to order v^7. Two different processes were considered. In the first one, the J/Ψ is singly produced,

$$e^- \ \text{Proton} \rightarrow e^- \ J/\Psi \ X \tag{3}$$

while in the second it is produced together with a light quark or gluon,

$$e^- \ \text{Proton} \rightarrow e^- \ g/q \ J/\Psi \ X \ . \tag{4}$$

The Feynman diagrams of the corresoponding photon parton subprocess are in the first case

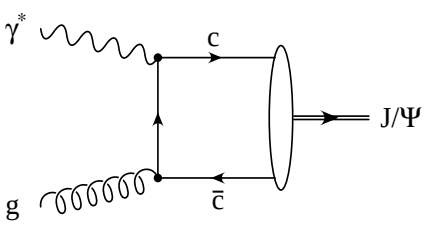

,

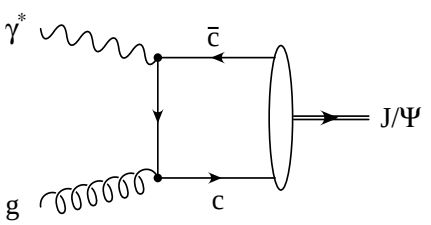

,

and in the second two representatives are

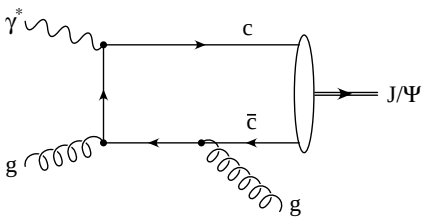

,

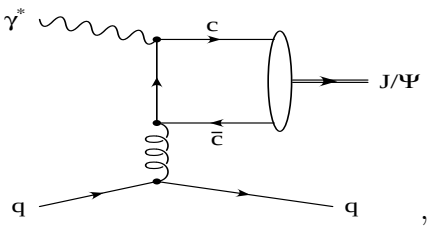

,

where γ^* stands for the virtual photon and g,q represents the gluon or light quark, respectively.

The relevant matrix elements up to order v^7 are:

	scaling
$\left\langle O^{J/\Psi}\left[1,^3S_1\right]\right\rangle$	$m_c^3 v^3$
$\left\langle O^{J/\Psi}\left[8,^1S_0\right]\right\rangle$	$m_c^3 v^7$
$\left\langle O^{J/\Psi}\left[8,^3S_1\right]\right\rangle$	$m_c^3 v^7$
$\left\langle O^{J/\Psi}\left[8,^3P_0\right]\right\rangle$	$m_c^3 v^7$

The calculation consists in the determination of the short distance coefficients $\hat{\sigma}\left(e^- \text{ Proton} \to \text{e}^- \text{ g/q c}\bar{\text{c}}\left[1/8,^{2\text{S}+1}\text{L}_\text{J}\right]\right)$ to these matrix elements. The underlying Feynman amplitude $\mathcal{M}$ is given by the conventional QCD Feynman rules. The heavy quark pair final state is defined by appropriate color and spin angular momentum projectors within the NRQCD projection formalism [7]. The proton initial state is accounted for by convoluting the partonic production cross section with the parton densities of the proton at the renormalization scale $m_{J/\Psi}^2 + Q^2$, $m_{J/\Psi}$ being the J/Ψ mass. Because of the nonabelian nature of QCD the treatment of the gluon polarization sum becomes somewhat tricky. Since different from the abelian case the relation $p_\mu \mathcal{M}^\mu = 0$, $\mathcal{M}$ being the gluon polarization vector amputated amplitude and p_μ the gluon momentum vector, does not hold in QCD, also the parts of $\sum_{\text{transversal polarizations}} \epsilon_\mu^*(p)\epsilon_\nu(p)$ proportional to p yield a nonvanishing contribution. As the full form of the sum over the transversal gluon polarizations

$$\sum_{\substack{\text{transversal}\\ \text{polarizations}}} \epsilon_\mu^*(p)\epsilon_\nu(p) = -g_{\mu\nu} + \frac{p_\mu n_\nu + p_\nu n_\mu}{pn} - \frac{n^2}{(pn)^2} p_\mu p_\nu \ ,$$

with n being an arbitrary space or lightlike vector satisfying $n\epsilon(p) = 0$, complicates the analytical calculation very much, the Slavnov Taylor identities were applied, which allow to replace $\sum_{\text{transversal polarizations}} \epsilon_\mu^*(p)\epsilon_\nu(p)$ simply by $-g_{\mu\nu}$, corresponding to a summation over all, not only transversal polarizations, and to compensate the contribution from the unphysical degrees of freedom by subtracting twice the amplitude squared with both

external gluons replaced by Fadeev Popov ghosts:

$$\sum_{\substack{\text{transversal}\\ \text{polarizations}}} |\mathcal{M}|^2 = \sum_{\substack{\text{all}\\ \text{polarizations}}} |\mathcal{M}|^2 - 2\,|\mathcal{M}|^2_{\substack{\text{external gluons}\\ \text{replaced by ghosts}}} \quad .$$

In the case of unpolarized J/Ψ production, the number of kinematical invariants can be reduced considerably by integrating out the azimuthal symmetry of the process in the photon parton center of mass frame. In this frame the only fixed vectors after the integration over the azimuthal angle Φ, defined as the angle between the leptonic plane, spanned by the incident and outgoing electron momenta k and k', and the hadronic plane, spanned by the in and outgoing parton momenta p and p', are the photon momentum q and the parton momentum p. This implies the general ansatz for the integrated lepton tensor

$$\int \frac{d\Phi}{2\pi} L_{\mu\nu} = a g_{\mu\nu} + b p_\mu p_\nu + c q_\mu q_\nu + d\,(p_\mu q_\nu + p_\nu q_\mu) \ ,$$

where the coefficients are determined by projecting the left hand side onto the basis tensors on the right hand side. It follows

$$\begin{aligned}\int \frac{d\Phi}{2\pi} L_{\mu\nu} = {} & \frac{1+(1-y)^2}{y^2}\left[-Q^2 g_{\mu\nu} + 4x^2 p_\mu p_\nu + 2x\,(p_\mu q_\nu + p_\nu q_\mu)\right] \\ & + \frac{4(1-y)}{y^2}\left[4x^2 p_\mu p_\nu + q_\mu q_\nu + 2x\,(p_\mu q_\nu + p_\nu q_\mu)\right] \ ,\end{aligned}$$

with $x = \frac{Q^2}{ys}$, $S = (P_p + k)^2$, P_p denoting the proton momentum, $Q^2 = -q^2$ being the photon virtuality and $y = \frac{P_p q}{P_p k}$ the energy fraction adopted by the photon from the electron in the proton rest frame. Besides y and the longitudinal momentum fraction ξ overtaken by the parton from the proton, the only remaining invariants are those of the photon parton subprocess

$$\begin{aligned}\hat{s} &= (p+q)^2 = \xi y S - Q^2 \\ Q^2 &= -q^2 \\ \hat{t} &= (p-p')^2 \\ \hat{u} &= (q-p')^2 \ .\end{aligned}$$

The first and the second part of the integrated lepton tensor can be interpreted as due to transversal and longitudinal polarization of the virtual photon respectively. This structure is directly carried over to the final analytic result for the J/Ψ production cross section

$$\frac{d\sigma}{d\xi dQ^2 dy dt} = \Gamma_T \frac{d\sigma_T}{d\xi dt} + \Gamma_L \frac{d\sigma_L}{d\xi dt} \ , \tag{5}$$

with the flux factors

$$\Gamma_T = \frac{\alpha}{2\pi Q^2}\frac{1+(1-y)^2}{y^2} \ ,$$

$$\Gamma_L = \frac{\alpha}{\pi Q^2}\frac{1-y}{y^2} \ ,$$

describing the content of transversally and longitudinally polarized photons in the electron. In the limit $Q^2 \to 0$, $\frac{d\sigma_T}{d\xi dt}$ becomes the differential photoproduction cross section while $\frac{d\sigma_L}{d\xi dt}$ vanishes. In the limit $v \to 0$, $\frac{d\sigma}{d\xi dQ^2 dy dt}$ reduces to the CSM result. The final analytic result was successfully tested in the photoproduction limit. Moreover it shows the correct factorization behaviour of the collinear divergencies.

This is now the place for a comparison with former literature results. Unless stated otherwise, it is refered to the process, in which the J/Ψ is produced together with an additional light parton. Concerning calculations within the CSM, analytic agreement with the photoproduction result of Berger and Jones [8] was found. For the deep inelastic regime $Q^2 > 0$, the longitudinal part of the cross sections presented by Krücker [9] and Guillet [10] show deviations from the one presented here by factors -1 and 2, respectively. In particular the differential production cross section of Guillet becomes negative for $y = 0.5$, $Q^2 = 25$ GeV^2, $\hat{t} = -10$ GeV^2. Absolutely no agreement was obtained with Merabet et. al. [11] and Körner et. al. [12]. Their results even do not satisfy the correct photoproduction limit. Regarding literature results within NRQCD, agreement was found with the photoproduction result of Ko, Lee and Song [13] as well as with the result of Mehen and Fleming [14] for the process e^- Proton $\to e^-$ J/Ψ X. Finally up to the $[8,^1S_0]$ contribution to the e^- $g \to e^-$ g J/Ψ X subprocess, no match was found with Yuan and Chao [15]. Their predictions for all other channels are not consistent with the above cited photoproduction results. Moreover their transversal $[8,^3S_1]$ and longitudinal $[8,^3P_J]$ contributions to the cross section of the partonic subprocess e^- $q \to e^-$ q J/Ψ suffer from mass dimensional inconsistencies.

3.2. The numerical calculation

Starting from the analytic result for the process e^- Proton $\to$ e$^-$ q/g J/Ψ the total cross section σ and the various differential distributions $\frac{d\sigma}{dQ^2}$, $\frac{d\sigma}{dz}$, $\frac{d\sigma}{dW}$, $\frac{d\sigma}{dy^*_{J/\Psi}}$, $\frac{d\sigma}{dp^*_T}$, $\frac{d\sigma}{dy_{J/\Psi}}$, $\frac{d\sigma}{dp^2_T}$ are numerically calculated. Thereby $z = \frac{P_p P_{J/\Psi}}{P_p q}$, $P_{J/\Psi}$ being the J/Ψ momrntum, is the inelasticity variable, defined as the energy fraction overtaken by the J/Ψ from the photon in the proton rest frame, $W^2 = (P_p + q)^2$ is the photon proton center of mass energy squared, $y^*_{J/\Psi}$, p^*_T are the J/Ψ rapidity and transversal momentum in the photon proton center of mass frame and $y_{J/\Psi}$, p_T are the J/Ψ rapidity and transversal momentum in the HERA laboratory frame. $y^*_{J/\Psi}$ and p^*_T are defined with respect to the photon proton collision axis in the photon proton center of mass frame while $y_{J/\Psi}$ and p_T are defined with respect to the electron proton collision axis in the HERA laboratory frame. Thereby the photon momentum in the first case and the electron momentum in the second is assumed to be oriented in positive z direction. $y^*_{J/\Psi}$ and p^*_T are then given by

$$y^*_{J/\Psi} = \frac{1}{2}\ln\frac{\hat{s}\left(m^2_{J/\Psi} - \hat{u}\right)}{\hat{s}\left(m^2_{J/\Psi} - \hat{t}\right) + Q^2 m^2_{J/\Psi}} + \frac{1}{2}\ln\frac{W^2}{\hat{s}} \ , \tag{6}$$

$$p_T^* = \frac{\sqrt{\hat{t}\left(\hat{s}\hat{u} + Q^2 m_{J/\Psi}^2\right)}}{\hat{s} + Q^2} \tag{7}$$

and $y_{J/\Psi}$ and p_T by

$$y_{J/\Psi} = y_{J/\Psi}^* + \ln\frac{(W^2+Q^2)m_T^*}{\sqrt{S}\ W\ m_T} + \frac{1}{2}\ln\frac{E_e}{E_p}\ , \tag{8}$$

$$p_T^2 = p_T^{*2} + A\left(A - 2p_T^*\cos\phi^*\right)\ , \tag{9}$$

where

$$A = \sqrt{\frac{Q^2\left(S - W^2 - Q^2\right)}{S\ W^2}}\ m_T^*\ \exp\left(y_{J/\Psi}^*\right)\ ,$$

$m_T^{*2} = m_{J/\Psi}^2 + p_T^{*2}$, ϕ^* are the transversal mass and the azimuthal angle of the J/Ψ in the photon proton center of mass frame and $m_T^2 = m_{J/\Psi}^2 + p_T^2$ is the J/Ψ transversal mass in the HERA laboratory frame. Furthermore, E_p and E_e are the proton and the electron energies in the HERA laboratory frame. Due to the azimuthal symmetry of the process the ϕ^* integration simply yields a factor 2π in calculating the distributions refering to the photon proton center of mass frame or those, which are Lorentz invariant. In the analytic result (5) this trivial integration has already been performed. In contrast, the ϕ^* integration becomes nontrivial in the HERA laboratory frame when calculating the distributions $\frac{d\sigma}{dy}$ and $\frac{d\sigma}{dp_T^2}$, since $y_{J/\Psi}$ and p_T depend on ϕ^*.

All the distributions were generated in form of histograms with the binnings adopted from the experimentalists [16]. The following cuts were imposed: $0.2 < z < 0.9$ to avoid collinear divergencies and diffractive contributions at $z \sim 1$ as well as effects from the breakdown of the NRQCD factorization at the edges of the phase space $z \sim 0$, $z \sim 1$ and 2 GeV^2 < Q^2 < 80 GeV^2, 40 GeV < W < 180 GeV to take the experimental range of acceptance into account. For the electron energy and the center of mass energy at HERA $E_e = 27.55$ GeV and $\sqrt{S} = 300$ GeV was taken. For the running QCD coupling the leading order formula was employed with the number of active flavours being $n_f = 3$. MRST98LO [17] with the QCD scale $\Lambda(3) = 224$ MeV was used for the parton densities and for the NRQCD matrix elements the recent values [18] $\left\langle O^{J/\Psi}\left[1,^3S_1\right]\right\rangle = 1.3$ GeV^3, $\left\langle O^{J/\Psi}\left[8,^3S_1\right]\right\rangle = 4.4\ 10^{-3}$ GeV^3, $\left\langle O^{J/\Psi}\left[8,^1S_0\right]\right\rangle = x\ M_r$, $\left\langle O^{J/\Psi}\left[8,^3P_0\right]\right\rangle = (1-x)M_r\frac{m_c}{r}$ were adopted, with the charm mass $m_c = 1.5$ GeV, $M_r = 8.7\ 10^{-2}$ GeV^3, $x = 0.5$ and $r = 3.4$. Thereby M_r is the usual linear combination $M_r = \left\langle O^{J/\Psi}\left[8,^1S_0\right]\right\rangle + \frac{r}{m_c^2}\left\langle O^{J/\Psi}\left[8,^3P_0\right]\right\rangle$. To estimate the error, the calculation was repeated for two further choices of the matrix elements $\left\langle O^{J/\Psi}\left[1,^3S_1\right]\right\rangle = 1.2\ ,\ 1.4$ GeV^3, $\left\langle O^{J/\Psi}\left[8,^3S_1\right]\right\rangle = 3.7\ 10^{-3}\ ,\ 5.1\ 10^{-3}$ GeV^3, the parameters x, M_r $x = 0\ ,\ 1\ ,$ $M_r = 7.8\ 10^{-2}\ ,\ 9.6\ 10^{-2}$ GeV^3, and the charm mass $m_c = 1.4\ ,\ 1.6$ GeV, according to a variation of all these parameters within their error bars. Moreover, the calculation was repeated for two further choices of the scale $\mu^2 = \frac{1}{2}\left(m_{J/\Psi}^2 + Q^2\right), 2\left(m_{J/\Psi}^2 + Q^2\right)$ and finally with CTEQ5L [19] as another choice of parton densities. When emploing CTEQ5L the values for the matrix elements were consistently changed [18] $\left\langle O^{J/\Psi}\left[1,^3S_1\right]\right\rangle = 1.4$ GeV^3, $\left\langle O^{J/\Psi}\left[8,^3S_1\right]\right\rangle = 3.9\ 10^{-3}$ GeV^3

and $M_r = 6.6\ 10^{-2}$. The QCD scale used in connection with CTEQ5L is $\Lambda(3) = 224$ MeV. The total error was then determined by Gaussian error propagation from the single variations of the numerical result due to the separate variation of the parton densities, the scale and the parameters.

3.3. Numerical results

In Figs. (1-7) the numerical results are presented and, as far as available, compared to the experimental data taken by the H1 collaboration at DESY HERA [16]. In each case, the predictions within the CSM (lower histogram) and within LO NRQCD (upper histogram) are shown. The experimental data clearly favour NRQCD against the CSM except for the case of the W distribution, where the data lie nearly in the middle between the CSM and the NRQCD results. Concerning the z distribution, the NRQCD calculation overshoots the data for high z values, which probably is due to the collinear singularity, occuring at $z = 1$ and a breakdown of the NRQCD factorization in this region. This discrepancy can be eliminated by a factorization of the collinear singularity into the parton density function of the proton and a resummation of higher order NRQCD effects, which become important near the boundary of the phase space [20]. To test the impact of the color octet mechanism, the ratio of the color singlet and the color octet contributions was studied. Distributions, for which this ratio becomes nearly constant, are not appropriate for probing the COM, because the color octet contribution could then be assigned to the color singlet channel by redefining the color singlet matrix element. This is only the case for the W distribution, where this ratio varies only very marginally between 0.33 and 0.34. The other distributions are very sensitive to the COM, showing a variation of this ratio between 0.31 and 0.45 (Q^2 distribution), 0.13 and 4.1 (z distribution), 0.19 and 1.5 (y^* distribution), 0.12 and 0.38 (p_T^{*2} distribution), 0.15 and 1.3 (y distribution) and finally 0.17 and 0.44 (p_T^2 distribution).

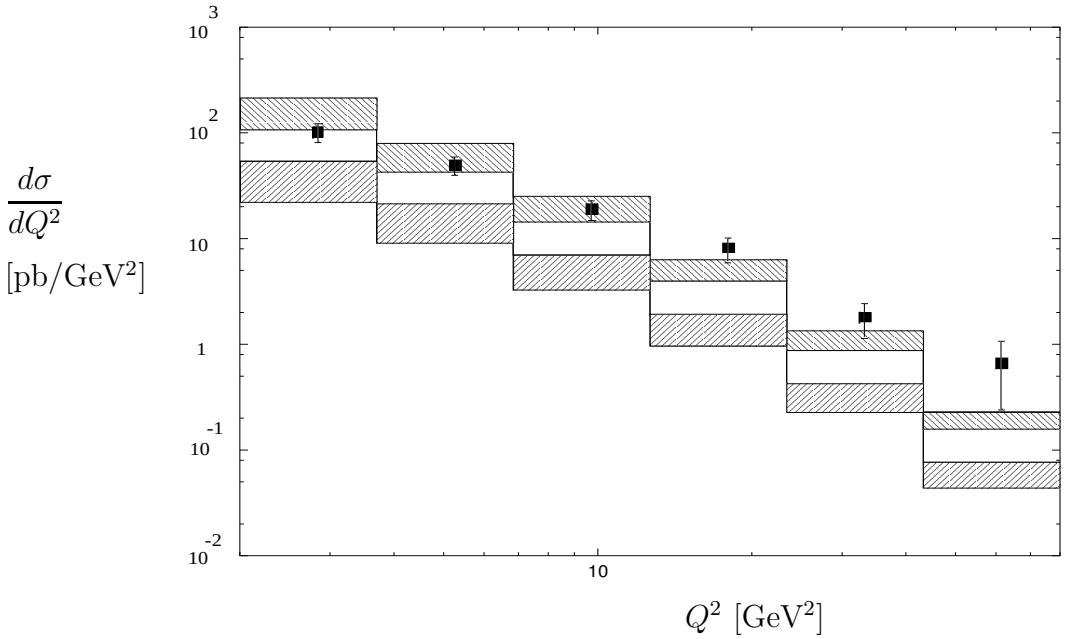

Figure 1. The Q^2 distribution of J/ψ inclusive production in ep DIS measured with the H1 detector [16] is compared with the LO NRQCD (upper histogram) and CSM (lower histogram) predictions.

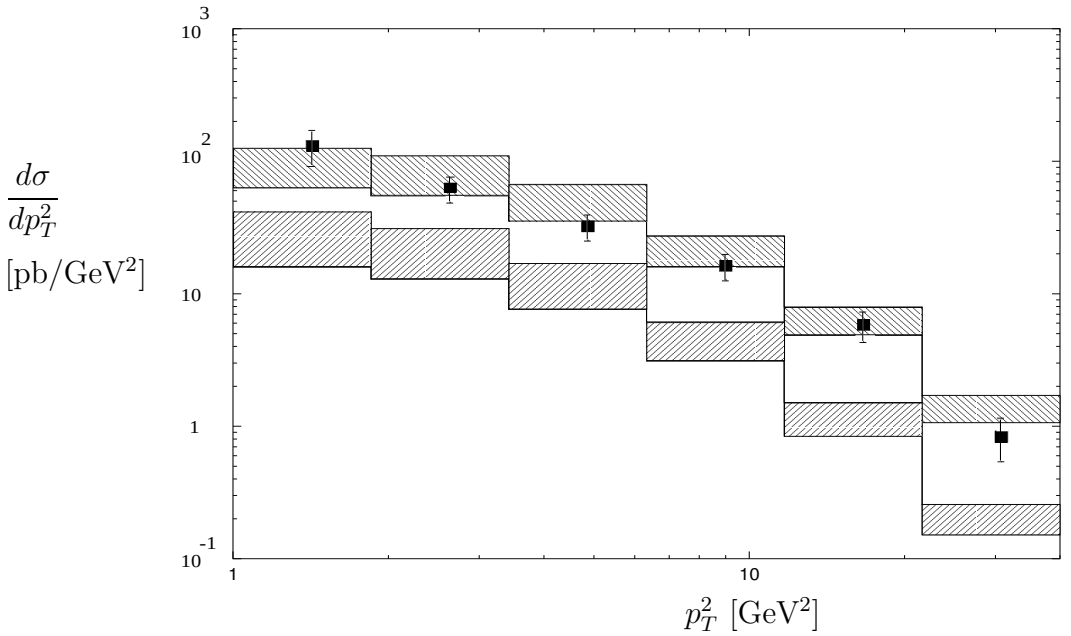

Figure 2. The p_T^2 distribution of J/ψ inclusive production in ep DIS measured with the H1 detector [16] is compared with the LO NRQCD (upper histogram) and CSM (lower histogram) predictions.

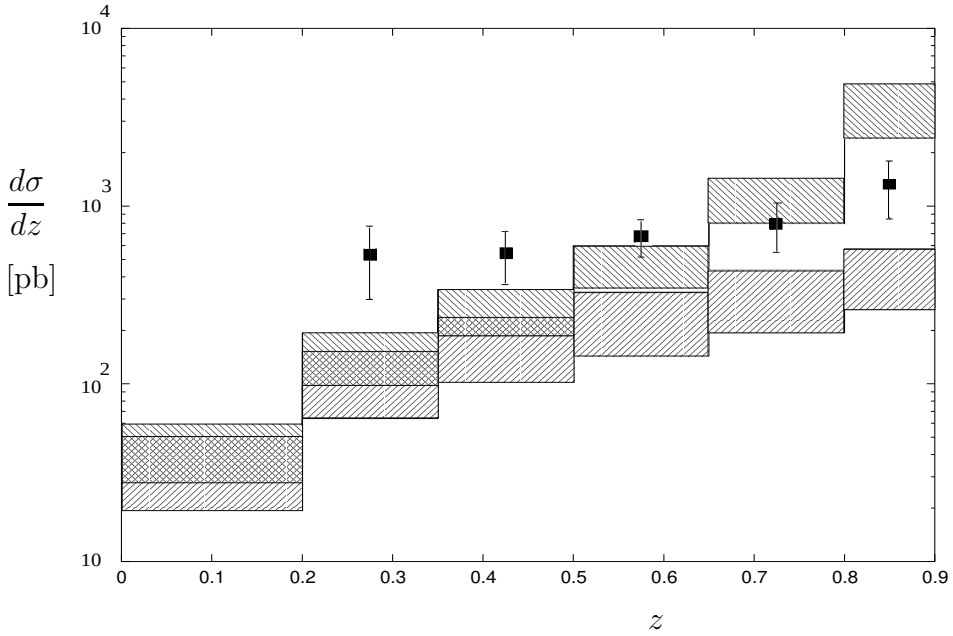

Figure 3. The z distribution of J/ψ inclusive production in ep DIS measured with the H1 detector [16] is compared with the LO NRQCD (upper histogram) and CSM (lower histogram) predictions.

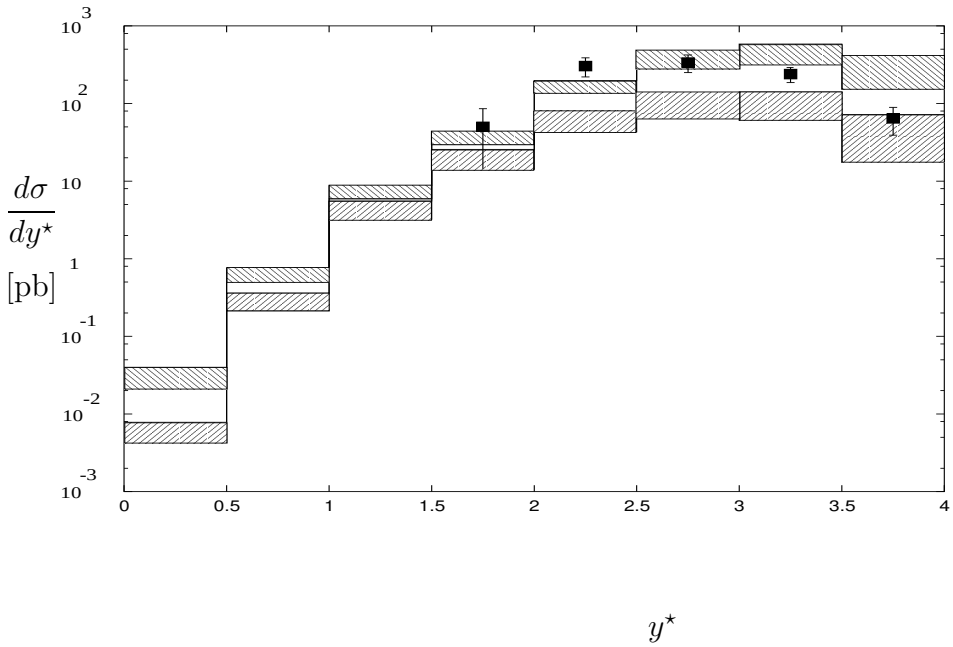

Figure 4. The $y^\star$ distribution of J/ψ inclusive production in ep DIS measured with the H1 detector [16] is compared with the LO NRQCD (upper histogram) and CSM (lower histogram) predictions.

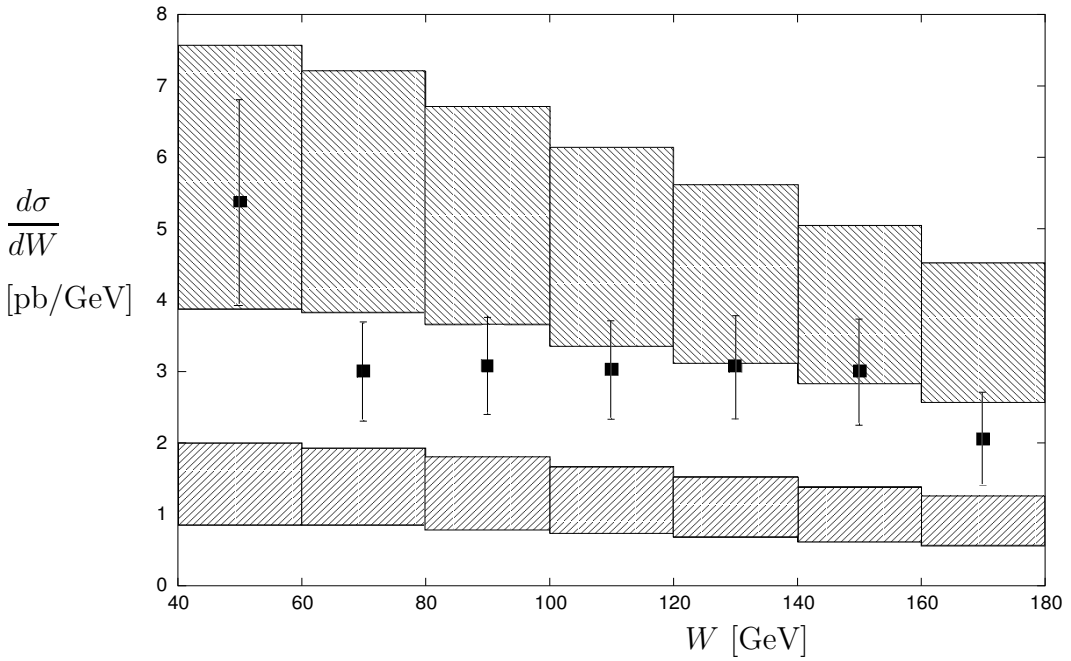

Figure 5. The W distribution of J/ψ inclusive production in ep DIS measured with the H1 detector [16] is compared with the LO NRQCD (upper histogram) and CSM (lower histogram) predictions.

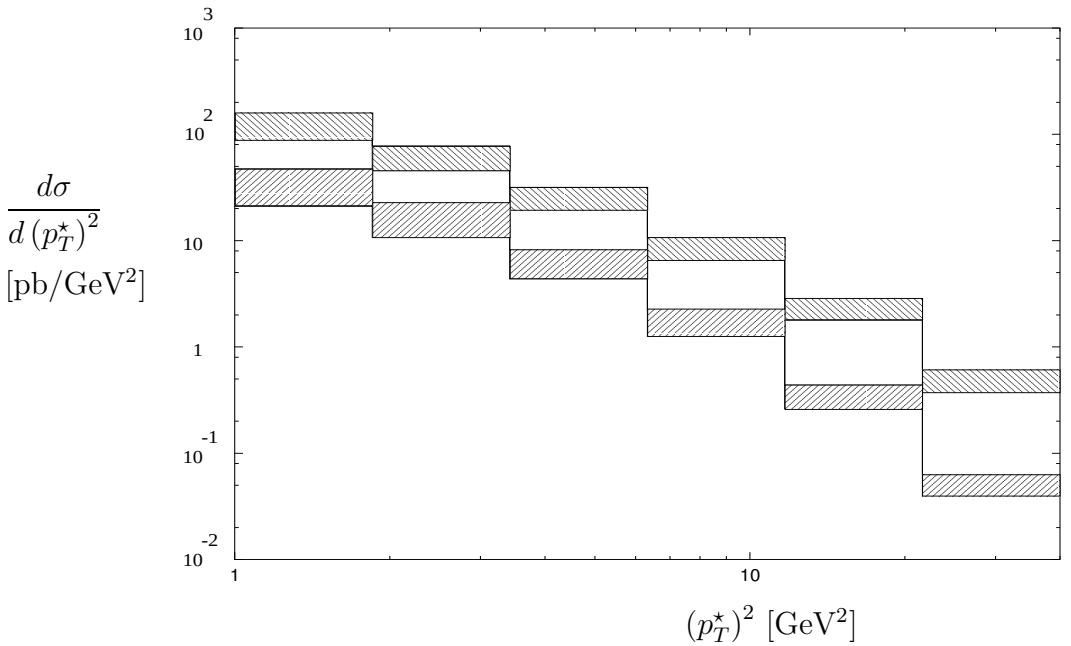

Figure 6. LO NRQCD (upper histogram) and CSM (lower histogram) predictions for the $(p_T^\star)^2$ distribution of J/ψ inclusive production in ep DIS.

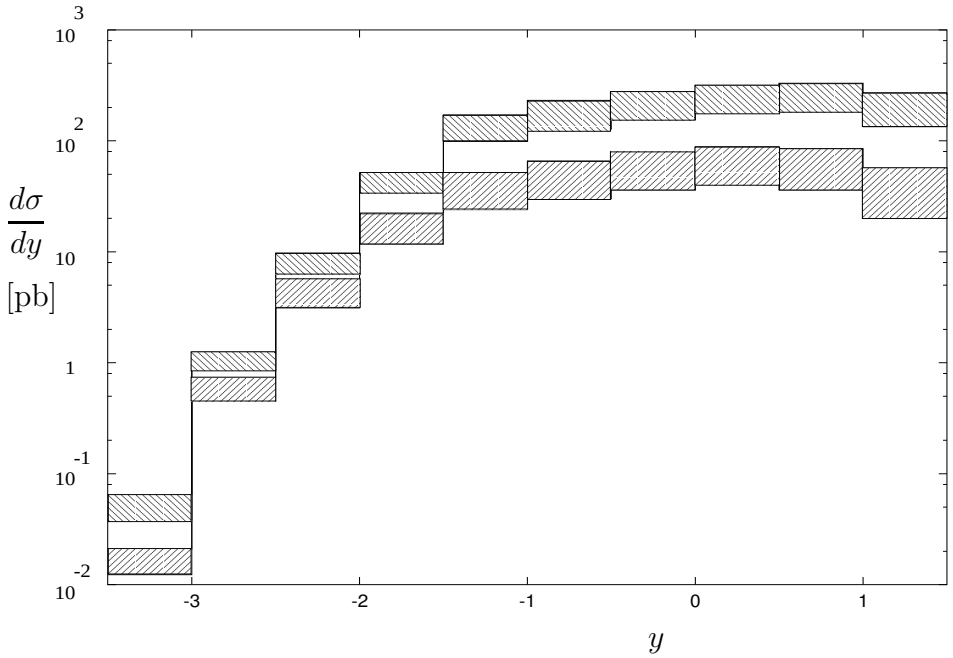

Figure 7. LO NRQCD (upper histogram) and CSM (lower histogram) predictions for the y distribution of J/ψ inclusive production in ep DIS.

4. Summary

Various differential distributions for J/Ψ electroproduction at DESY HERA were calculated and compared to experimental data. NRQCD was found to describe the data significantly better than the CSM. In addition, the sensitivity of various distributions to the COM was studied. If realized in nature, the COM should manifestly affect the distributions in the J/Ψ rapidity, the J/Ψ transversal momentum as well as in the photon virtuality and the inelasticity variable. The differential distribution in W is rather inappropriate for testing the COM.

Acknowledgements

I am indebted to my supervisor B.A. Kniehl. This work was supported by the Studienstiftung des Deutschen Volkes through a PhD scholarship.

References

[1] B.A. Kniehl and L. Zwirner, Report No. DESY 01-146 MPI/PhT/2001-29, Nucl. Phys. (to appear)
[2] R. Baier, R. Rückl, Phys. Lett. 102 B (1981) 364; Z. Phys. C 19 (1983) 251; B. Humpert, Phys. Lett. B 184 (1987) 105; R. Gastmans, W. Troost, T.T. Wu, Phys. Lett. B 184 (1987) 257; Nucl. Phys. B 291 (1987) 731.

[3] G.T. Bodwin, E. Braaten, G.P. Lepage, Phys. Rev. D 51 (1995) 1125; Phys. Rev. D 55 (1997) 5853 (Erratum).
[4] CDF Collaboration, F. Abe et al., Phys. Rev. Lett. 69 (1992) 3704; Phys. Rev. Lett. 71 (1993) 2537; Phys. Rev. Lett. 79 (1997) 572; Phys. Rev. Lett. 79 (1997) 578; D0 Collaboration, S. Abachi et al., Phys. Lett. B 370 (1996) 239; D0 Collaboration, B. Abbott et al., Phys. Rev. Lett. 82 (1999) 35.
[5] E.Braaten and T.C.Yuan, Phys. Rev. Lett. 71, 1673 (1993)
[6] G.T.Bodwin, E.Braaten, and G.P.Lepage, Phys. Rev. D 46, R1914 (1992)
[7] A. Petrelli, M. Cacciari, M. Greco, F. Maltoni, M.L. Mangano, Nucl. Phys. B 514 (1998) 245;
[8] E.L. Berger, D. Jones, Phys. Rev. D 23 (1981) 1521.
[9] D. Krücker, PhD Thesis, RWTH Aachen, 1995.
[10] J.-Ph. Guillet, Z. Phys. C 39 (1988) 75.
[11] H. Merabet, J.F. Mathiot, R. Mendez-Galain, Z. Phys. C 62 (1994) 639.
[12] J.G. Körner, J. Cleymans, M. Kuroda, G.J. Gounaris, Phys. Lett. 114B (1982) 195.
[13] P. Ko, J. Lee, H.S. Song, Phys. Rev. D 54 (1996) 4312; Phys. Rev. D 60 (1999) 119902 (Erratum).
[14] S. Fleming, T. Mehen, Phys. Rev. D 57 (1998) 1846;
[15] F. Yuan, K.-T. Chao, Phys. Rev. D 63 (2001) 034017.
[16] A. Meyer, PhD Thesis, Universität Hamburg, 1998, Report No. DESY-THESIS-1998-012; S. Mohrdieck, private communication.
[17] A.D. Martin, R.G. Roberts, W.J. Stirling, R.S. Thorne, Eur. Phys. J. C 4 (1998) 463.
[18] E. Braaten, B.A. Kniehl, J. Lee, Phys. Rev. D 62 (2000) 094005.
[19] CTEQ Collaboration, H.L. Lai et al., Eur. Phys. J. C 12 (2000) 375.
[20] M. Beneke, I.Z. Rothstein and M.B. Wise, Phys.Lett.B408:373-380,1997